Letter

Exceptional dynamics of interacting spin liquids

Kang Yang,[1] Daniel Varjas,[1] Emil J. Bergholtz,[1] Sid Morampudi,[2] and Frank Wilczek[1,2,3,4,5]

[1]*Department of Physics, Stockholm University, AlbaNova University Center, 106 91 Stockholm, Sweden*

[2]*Center for Theoretical Physics, Massachusetts Institute of Technology, Cambridge, Massachusetts 02139, USA*

[3]*T. D. Lee Institute, Shanghai 201210, China*

[4]*Wilczek Quantum Center, Department of Physics and Astronomy, Shanghai Jiao Tong University, Shanghai 200240, China*

[5]*Department of Physics and Origins Project, Arizona State University, Tempe, Arizona 25287, USA*

(Received 14 February 2022; accepted 29 September 2022; published 14 November 2022)

We show that interactions in quantum spin liquids can result in non-Hermitian phenomenology that differs qualitatively from mean-field expectations. We demonstrate this in two prominent cases through the effects of phonons and disorder on a Kitaev honeycomb model. Using analytic and numerical calculations, we show the generic appearance of exceptional points and rings depending on the symmetry of the system. Their existence is reflected in dynamical observables including the dynamic structure function measured in neutron scattering. The results point to different phenomenological features in realizable spin liquids that must be incorporated into the analysis of experimental data and also indicate that spin liquids could be generically stable to wider classes of perturbations.

DOI: 10.1103/PhysRevResearch.4.L042025

Quantum spin liquids are low-temperature phases of matter in which quantum fluctuations prevent the establishment of long-range magnetic order. Besides the absence of local order, a more distinct characteristic is the presence of exotic fractionalized spin excitations (spinons) and emergent gauge fields [1–4] due to long-range entanglement in the system. This suggests possible applications ranging from quantum simulation to spintronics [5].

Much recent work has focused on realizing new types of spin liquids and understanding their implications in dynamics and experiments through mean-field approaches. Interactions and disorder are prominent in many experimental settings, however, and can affect the dynamics and thermodynamics [6–18]. A common expectation is that such effects either renormalize the properties of quasiparticles (and give them finite lifetimes), or open a gap if they violate certain symmetries. Here, we explore an intriguing alternative route where interactions and disorder can generically lead to qualitatively different phenomena, through distinct non-Hermitian effects that depend on the symmetries of the interactions [19–29]. These non-Hermitian components can induce a unique level attraction in contrast with the usual band degeneracies of Hermitian perturbations. We will illustrate this general principle in the context of the Kitaev honeycomb model, which has received much attention recently in view of potential experimental realizations [30–39], whereas our symmetry analysis may apply to a variety of models. The presence of disorder and phonons can lead to the appearance of so-called exceptional rings and exceptional points which possess an unusual square-root dispersion [40,41]. This results in unusual features in experimental observables including asymmetric Fermi arcs, which cannot be achieved generically in Hermitian settings. The resulting generic phenomena also illustrate that spin liquids can be stable to a wider variety of perturbations and are less fragile and richer than typically assumed.

Effective non-Hermitian description. Elucidating the subtle signatures of a spin liquid in experiments requires an understanding of dynamical observables such as the spectral function and dynamic structure factor. Linear response connects these observables to tangible measurements such as scattering cross sections. Calculating these observables in interacting systems is not easy, although they have been quantified in some crucial cases such as an interacting electron gas (Fermi-liquid theory).

A fundamental object to calculate dynamical observables is the Green's function where interactions are accounted for through a self-energy. The Green's function for an interacting or disordered system satisfies the Dyson equation $[\omega - H_0 - \Sigma^{A/R}(\omega)]G^{A/R}(\omega) = I$, where I is the identity operator and H_0 is the unperturbed Hamiltonian, and the superscripts A, R refer to advanced or retarded. The retarded version is appropriate for calculating the time evolution of simply specified initial ("in") states. The self-energy $\Sigma^{A/R}(\omega)$ terms are induced by the interaction or the disorder. The Green's function has poles at $\omega = E$ whenever $\det[E - H_0 - \Sigma^{A/R}(E)] = 0$. At low energy, the self-energy can be expanded in powers of ω, $\Sigma^R(\omega) = \Sigma^R(0) + \omega\Sigma^{(1)} + \cdots$. Unlike the original Hamiltonian, the self-energy is usually not Hermitian [42]. We denote the Hermitian and anti-Hermitian component of the self-energy as $\bar{\Sigma}$ and $\tilde{\Sigma}$. The linear term $\Sigma^{(1)}$ plays an important role in wave-function renormalization and friction

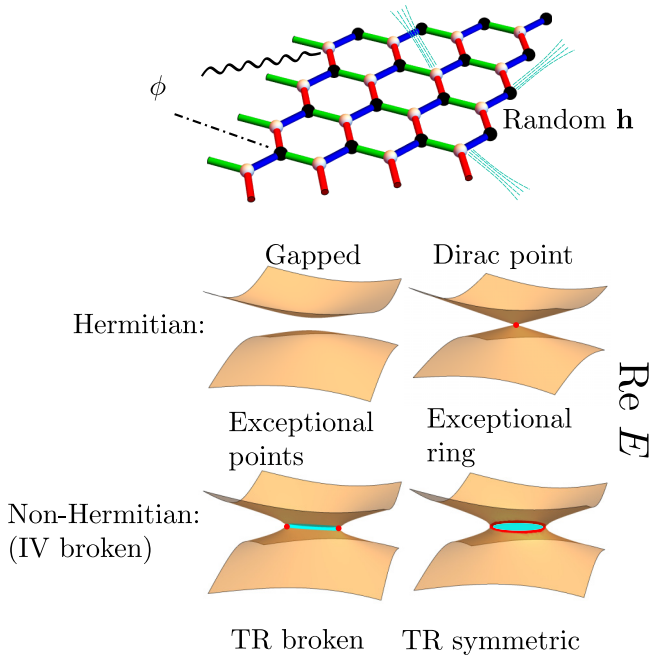

FIG. 1. The Kitaev honeycomb model with interactions carried by a bosonic field or bond disorders. Depending on whether inversion (IV) symmetry and time-reversal (TR) symmetry are preserved, we can have different types of non-Hermitian phases or a trivial gapped phase. The real parts of the "energy" difference ΔE (yellow) between the two Majorana bands are shown as a function of momenta for different scenarios.

for bosonic operators [43]. Here, we assume $||\Sigma^{(1)}|| \ll 1$ and neglect it for simplicity. The leading-order term in the Dyson equation can be treated as an effective Hamiltonian $H^{\text{eff}} = H + \Sigma^R(0)$.

Symmetries of interactions and exceptional degeneracies. This effective Hamiltonian is usually non-Hermitian and can exhibit "exceptional" degeneracies in its spectrum depending on the symmetries obeyed by the interactions [44–46]. We illustrate this through the Kitaev honeycomb model.

The Kitaev honeycomb model [47] is defined through compass interactions linking directions in spin space and real space of spin-1/2,

$$H_0 = -\sum_{\langle jk\rangle_\alpha} J_\alpha \sigma_j^\alpha \sigma_k^\alpha, \tag{1}$$

where $\langle jk\rangle_\alpha$ labels the lattice (Fig. 1) and $\alpha = x, y, z$ labeling the three types of links of a hexagonal lattice with σ^α the corresponding Pauli matrices. At low energies, the system is effectively described by Majorana quasiparticles c_a with a Dirac dispersion interacting with a $\mathbb{Z}_2$ gauge field, where a labels the two sublattice indices.

The Majorana operators always possess a particle-hole symmetry, $Cc_{a,\mathbf{k}}C^{-1} = c_{a,-\mathbf{k}}$, reflecting the underlying real bosonic spin degrees of freedom. The honeycomb lattice is inversion invariant: Under inversion transformation, the two orbitals are interchanged while the $\mathbb{Z}_2$ gauge field coupling the two orbitals obtains a minus sign. Therefore the Majorana operators transform as $\mathcal{P}c_{a,\mathbf{k}}\mathcal{P}^{-1} = \sum_b \varepsilon_{ab} c_{b,-\mathbf{k}}$. The time-reversal symmetry is crucial in protecting the gapless phase. The transformation rule is given by $\mathcal{T}c_{1,\mathbf{k}}\mathcal{T}^{-1} = c_{1,-\mathbf{k}}$, $\mathcal{T}c_{2,\mathbf{k}}\mathcal{T}^{-1} = -c_{2,-\mathbf{k}}$. With these rules, we can explicitly compute how the self-energy transforms under $\mathcal{T}$, $\mathcal{P}$, and $\mathcal{C}$. They are summarized in Table I.

From these symmetries, we find different types of exceptional degeneracies. We first look at particle-hole (PH) symmetry and inversion symmetry. PH symmetry requires the non-Hermitian (NH) component of the self-energy to satisfy $\tilde{\Sigma}^R_{ab}(\omega, \mathbf{k}) = \tilde{\Sigma}^R_{ba}(-\omega, -\mathbf{k})$. Inversion symmetry imposes $\tilde{\Sigma}^R_{22}(\omega, \mathbf{k}) = \tilde{\Sigma}^R_{11}(\omega, -\mathbf{k})$ and $\tilde{\Sigma}^R_{12}(\omega, \mathbf{k}) = -\tilde{\Sigma}^R_{21}(\omega, -\mathbf{k})$. So when both of them are present, the NH self-energy can only be proportional to an identity matrix at $\omega = 0$, $\tilde{\Sigma}^R_{ab}(0, \mathbf{k}) = \delta_{ab}\tilde{\Sigma}^R(0, \mathbf{k})$. Under this circumstance, the NH components are trivial, merely broadening the resonance peaks of the Majorana operators. So in order for a nontrivial NH self-energy, we need to break either PH or inversion symmetry. The former is an intrinsic property of Majorana operators. Thus we can only choose to break the inversion symmetry.

Looking at the time-reversal symmetry, it requires $\tau_z \Sigma^R(\omega, \mathbf{k})\tau_z = [\Sigma^A(\omega, -\mathbf{k})]^*$ with $\tau_z = \text{diag}(1, -1)$ the z-Pauli matrix. Together with PH symmetry, we find that time-reversal symmetry implies $\bar{\Sigma}^R_{aa}(0, \mathbf{k}) = 0$ and $\tilde{\Sigma}^R_{ab}(0, \mathbf{k}) = 0 (a \neq b)$. We can only have purely imaginary numbers in the diagonals of $\Sigma^R(0, \mathbf{k})$ when time-reversal symmetry is present.

With the symmetry restrictions, we discuss the topology of band touchings. The Majorana Hamiltonian can be expressed in terms of the Pauli matrices $H_m = d_0 I + \mathbf{d} \cdot \boldsymbol{\tau}$. The d_0 vector merely shifts the touching energy level and we only need to focus on $E = \pm\sqrt{\mathbf{d} \cdot \mathbf{d}}$. When the system preserves time-reversal symmetry, we have $d_z = i\tilde{d}_z$ and $d_{x/y} = \bar{d}_{x/y}$. So we have

$$E(\mathbf{k}) = \pm\sqrt{\bar{d}_x^2(\mathbf{k}) + \bar{d}_y^2(\mathbf{k}) - \tilde{d}_z^2(\mathbf{k})}. \tag{2}$$

Now the energy vanishes at $\bar{d}_x^2(\mathbf{k}) + \bar{d}_y^2(\mathbf{k}) = \tilde{d}_z^2(\mathbf{k})$ and is purely imaginary when $\bar{d}_x^2(\mathbf{k}) + \bar{d}_y^2(\mathbf{k}) < \tilde{d}_z^2(\mathbf{k})$. The solution to $\bar{d}_x^2(\mathbf{k}) + \bar{d}_y^2(\mathbf{k}) = \tilde{d}_z^2(\mathbf{k})$ is a one-dimensional (1D) closed curve, the exceptional curve. Inside the exceptional curve, the energy is purely imaginary; the system is gapless for the real part of the energy. When the time-reversal symmetry is lifted, the system usually possesses a gap $\Delta \sim \min\sqrt{\bar{d}^2(\mathbf{k})}$. However, the inclusion of a nontrivial NH term can change the situation. The energy is given by

$$E(\mathbf{k}) = \pm\sqrt{\bar{d}^2(\mathbf{k}) - \tilde{d}^2(\mathbf{k}) + 2i\bar{\mathbf{d}}(\mathbf{k}) \cdot \tilde{\mathbf{d}}(\mathbf{k})}. \tag{3}$$

By dimension counting, the imaginary and real parts in the square root can vanish robustly at an isolated point $\mathbf{k} = \mathbf{k}_*$ since these are two restrictions for a two-dimensional (2D) problem. This is different from the Hermitian case where all the three components d_x, d_y, and d_z must vanish. The NH components generate a level attraction and may close the (real) gap, leading to an exceptional point at $\mathbf{k}_*$.

Exceptional points are general features of NH effective Hamiltonians. However, the exceptional point itself is not directly reflected in the single-body spectral function. The existence of exceptional points is always accompanied by Fermi arcs. Compared to the Dirac point, the Fermi arc is extensive in one direction while narrow in the orthogonal direction. Its

TABLE I. Summary of symmetries. We use a general complex fermion notion. For Majorana operators used here, we need to substitute $\psi_{a,\mathbf{k}} = c_{a,\mathbf{k}}$, $\psi^\dagger_{a,\mathbf{k}} = c_{a,-\mathbf{k}}$.

Symmetry of Green's functions		
Time reversal	Particle-hole	Inversion
$\mathcal{T}\psi_{a,\mathbf{k}}\mathcal{T}^{-1} = \sum_b U_{ab}\psi_{b,\mathbf{k}}$ $\Sigma^R_{ab}(\omega,\mathbf{k}) = \sum_{cd} U_{ac}U^*_{bd}[\Sigma^A_{cd}(\omega,-\mathbf{k})]^*$ $E(\mathbf{k}) \to E(-\mathbf{k})$	$\mathcal{C}\psi_{a,\mathbf{k}}\mathcal{C}^{-1} = \psi^\dagger_{a,-\mathbf{k}}$ $\Sigma^R_{ab}(\omega,\mathbf{k}) = -\Sigma^A_{ba}(-\omega,-\mathbf{k})$ $E(\mathbf{k}) \to -E^*(-\mathbf{k})$	$\mathcal{P}\psi_{a,\mathbf{k}}\mathcal{P}^{-1} = \sum_b U^I_{ab}\psi_{b,-\mathbf{k}}$ $\Sigma^R_{ab}(\omega,\mathbf{k}) = \sum_{cd} U^I_{ac}U^{I*}_{bd}\Sigma^R_{cd}(\omega,-\mathbf{k})$ $E(\mathbf{k}) \to E(-\mathbf{k})$

effective dispersion is also biased at finite frequency (see Supplemental Material [48]). Such a highly anisotropic feature could be observed in inelastic neutron scattering. *Exceptional rings in a disordered Kitaev honeycomb model*. Now we specialize to the Kitaev honeycomb model, a $\mathbb{Z}_2$ spin liquid with Dirac cones. We find that including disorder respecting time reversal on average and breaking inversion symmetry realizes a phase with degeneracies on, and square-root dispersion near, the exceptional rings.

We consider a random magnetic field with zero average. This type of disorder is different from vacancies [49,50], random vortex backgrounds [51], or nearest-neighbor exchange disorders [52,53] that have been considered previously in the literature. We treat the random magnetic field perturbatively, assuming that the ground state remains in the zero flux sector. As explained in the Supplemental Material (SM) [48], this results (at lowest orders) in a Majorana hopping model with disordered first- and second-neighbor hoppings. The model preserves time-reversal symmetry on average. To observe exceptional rings, we break inversion symmetry by allowing different magnitudes of the random external field on the two sublattices. This can be achieved experimentally by proximity coupling to a paramagnetic substrate with inequivalent atoms near the two sublattices.

As the symmetry analysis shows, we need to break inversion symmetry. This can be done by introducing a disorder potential for the next-nearest hopping amplitudes of the Majorana modes on orbital 1, $iV_{\mathbf{l}}(\mathbf{r})\psi_1(\mathbf{r}+\mathbf{l})\psi_1(\mathbf{r})$, where the hopping vector can be $\mathbf{l} = \mathbf{a}_1, \mathbf{a}_2, \mathbf{a}_1+\mathbf{a}_2$. This term breaks time-reversal symmetry while the exceptional rings require time-reversal symmetry. The strategy is to preserve this symmetry in average. That is to say, the statistical average of the time-reversal breaking term vanishes $\langle V_{\mathbf{l}}(\mathbf{r})\rangle = 0$. We show in SM [48] that the transformation rules in Table I still apply. The disorder is assumed to be uncorrelated at different sites $\langle V_{\mathbf{l}}(\mathbf{r})V_{\mathbf{l}'}(\mathbf{r}')\rangle = -F^{\mathbf{l}}\delta_{\mathbf{l},\mathbf{l}'}\delta(\mathbf{r}-\mathbf{r}')$. The self-consistent Born approximation reads as

$$\Sigma^R_{11}(\omega,\mathbf{k}) = -\sum_{\mathbf{k}',\mathbf{l}}[1-e^{-i(\mathbf{k}+\mathbf{k}')\cdot\mathbf{l}}]F^{\mathbf{l}}(\mathbf{k}-\mathbf{k}')G_{11}(\omega,\mathbf{k}'). \tag{4}$$

If $\tilde{d}_0$ is taken to be infinitesimal, the NH part of the above equation vanishes as $\omega \to 0$. To circumvent this situation, we may consider including a finite $\tilde{d}_0$ brought by other inversion-symmetry preserving mechanisms, such as nearest-neighbor Majorana disorder potentials. This type of disorder brings a small finite lifetime to the Majorana excitations.

In Figs. 2(c) and 2(d) we show the resulting effective Hamiltonian, with clear evidence of an exceptional ring around the K points. We also show the single Majorana spectral function in Figs. 2(a) and 2(b), with signatures of a zero-frequency drumhead state inside the exceptional ring. Somewhat surprisingly, the total density of states, shown in Fig. 2(e), has a dip, instead of a peak at zero energy. This is a consequence of a strong suppression of the zero-frequency spectral weight outside the exceptional ring (ER), combined with the larger available phase space outside the ER, allowing the finite-frequency density of states to surpass the zero frequency value.

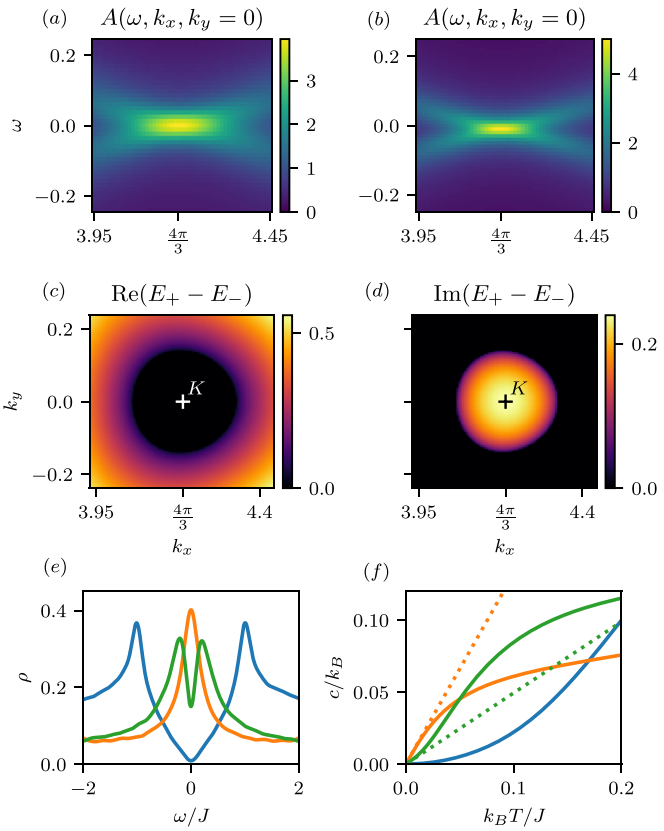

FIG. 2. Exceptional ring in a disordered Kitaev honeycomb model. Spectral function along the $k_y = 0$ cut from (a) disordered numerics and (b) SCBA. (c) Real and (d) imaginary part of the gap in the effective Hamiltonian near the K point. The real gap vanishes inside, the imaginary gap outside the exceptional ring. (e) Density of states and (f) specific heat for clean (blue), nearest-neighbor disordered without exceptional ring (orange), and second-neighbor disordered with exceptional ring (green) systems, the low-temperature linearized specific heat with dotted lines.

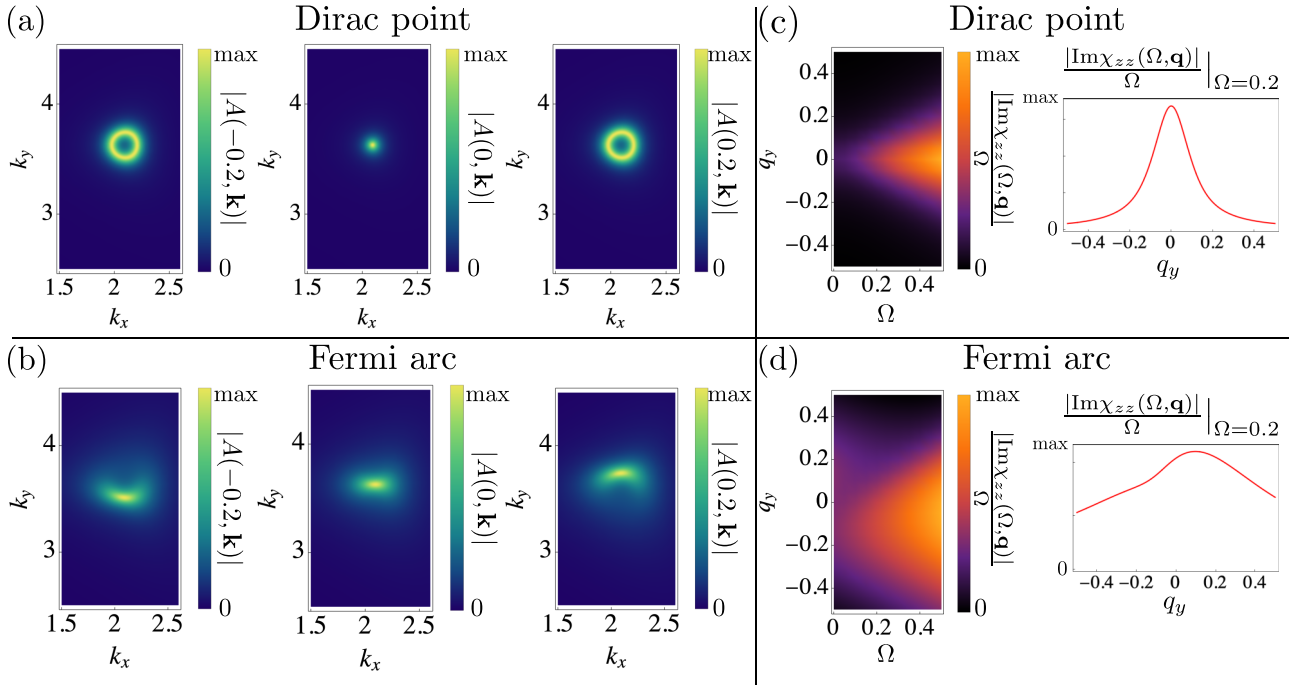

FIG. 3. The spectral functions of Majorana excitations $A(\omega,\mathbf{k}) = -\mathrm{tr}[G^R(\omega,\mathbf{k}) - G^{R\dagger}(\omega,\mathbf{k})]/(2i\pi)$, and their spin structure factors in the presence of Heisenberg and cross-term interactions. The energy unit is J. (a)–(c) The Dirac point for Hermitian systems. The single-particle spectral function is supported at a point. The spin structure factor as a function of the frequency Ω and momentum $\mathbf{q}$ takes a conic structure for both the $\mathbf{q}_x$-direction cut and the $\mathbf{q}_y$-direction cut. (c)–(f) A Fermi arc with NH components $\tilde{d}_0 = -0.35J$, $\tilde{d}_x = 0.25J$, associated with the exceptional points in the single-body Majorana spectral function. The spin structure is now anisotropic due to the strong asymmetric behaviours of the Fermi arc. (g), (h) The spectral functions of the Fermi arc at finite positive and negative frequencies. The Fermi arc becomes convex at finite frequencies. The direction of the deformation depends on the sign of the frequency. (i) The cuts of the spin structure factor at $\Omega = 0.2J$ along $(0, q_y)$ and $(q_x, 0)$.

To support the self-consistent Born approximation (SCBA) results, we use the kernel polynomial method [54,55] to approximate the disorder-averaged retarded Green's function $\langle G^R_{ab}(\omega,\mathbf{k})\rangle_{\mathrm{dis}}$ numerically. From this, we obtain the self-energy, the effective Hamiltonian, and the single-particle and two-particle spectral functions, which all show excellent agreement with the SCBA results. (For details, see SM [48].) We also show a comparison of the density of states and specific heat [56,57] for the clean, nearest-neighbor disordered (without exceptional ring) and second-neighbor disordered (with exceptional ring) systems in Figs. 2(e) and 2(f). The key difference between the two disordered cases is the opposite deviation from the linearized low-temperature specific heat. This can be understood using Fermi-liquid theory and Sommerfeld expansion: The linear term is only sensitive to the zero-frequency density of states, however, the sign of the cubic term depends on whether zero frequency is a minimum or a maximum of the density of states. (For details, see SM [48].)

Exceptional points and Fermi arcs in a Kitaev honeycomb model interacting with phonons. We show here that a $\mathbb{Z}_2$ spin liquid with Dirac cones when coupled to gapped excitations such as optical phonons [58] instead can realize a qualitatively different phase with pointlike exceptional degeneracies connected by Fermi-arc degeneracies in the real part of the spectrum. The phonon couplings can be generated by considering vibrations of ions around their equilibrium positions [59,60]. A spin-spin interaction can be generally written as $\sum_{\mathbf{r}_1,\alpha,\ldots} J_{\alpha,\beta,\ldots}(\mathbf{r}_1,\mathbf{r}_2,\ldots)\sigma^\alpha_{\mathbf{r}_1}\sigma^\beta_{\mathbf{r}_2}\cdots$. At the equilibrium position $\mathbf{r}_j = \mathbf{r}^{(0)}_j$, we should have $J_{\alpha,\beta,\ldots}(\mathbf{r}^{(0)}_1,\mathbf{r}^{(0)}_2,\ldots) = 0$ except for those J belonging to the Kitaev interaction. For small ion vibrations, we have the phonon-spin interaction $\sum_{\mathbf{r}_1,\alpha,j,\ldots} \partial_{\mathbf{r}_j} J_{\alpha,\beta,\ldots}(\mathbf{r}^{(0)}_1,\mathbf{r}^{(0)}_2,\ldots)\delta\mathbf{r}_j\sigma^\alpha_{\mathbf{r}_1}\sigma^\beta_{\mathbf{r}_2}\cdots$. These spin operators can be written in terms of Majorana operators. The low-energy physics is obtained by those do not excite $\mathbb{Z}_2$ vortices. For example, a nearest-neighbor Kitaev coupling gives phonons coupled to the different species of Majorana operators $\phi c_1 c_2$ and a three-spin coupling can lead to phonons coupled to the same species of Majorana operators $\phi c_1 c_1$.

In order to have interesting exceptional degeneracies we need to break inversion symmetry. This can be achieved by giving different couplings to the two sublattices of the honeycomb model. For phonons, this will lead to asymmetric couplings between their normal modes and the two species of Majorana modes. In order to break time-reversal symmetry, we require couplings of the form $\phi c_1 c_1$.

In the presence of a Heisenberg interaction and cross interaction, the spin operator gets mixed with the low-energy Majorana operator directly [61]. The spin response function can be evident even below the flux gap temperature. We compute the behaviors of the spin structure factor in Fig. 3. When the Fermi arc is present, the spin structure constant develops very different directional-dependent shapes compared to the Dirac cones. The cut along the y direction is biased while the cut along the x direction is uniformly broadened for Fermi arcs. This is very different

from the naive isotropic conic structure for Dirac-Majorana dispersion.

Discussion. The Kitaev honeycomb model is the subject of much recent interest due to prominent experimental candidates such as α-$RuCl_3$ [30–39]. Recent studies have shown that phonons can play a significant role in the experimental setting [58–60]. In this model, the optical phonon energy is well above the flux gap, and the signature of exceptional points may be obscured by the effective flux disorders. From our symmetry analysis, we may instead break the inversion symmetry by various means such as stacking the 2D material on a substrate which does not have such a symmetry. The exceptional ring could also be realized by depositing the material on a substrate with random magnetic disorder. Besides measurement of the dynamic structure factor, recent techniques using nonlinear spectroscopy [62–66] could also provide a more direct probe of the single-particle properties which would more directly reveal the exceptional degeneracies.

Our results point to different phenomena in spin liquids depending on the symmetries of the interactions and kinds of disorder present in them. One might have feared that those complications would obfuscate the signature of the spin liquid. Instead, we suggest that it leads to distinctive exceptional degeneracies observable in experimental settings. As our symmetry study works for generic fermionic excitations, the exceptional point and ring can also emerge in other 2D strongly interacting systems. And its generalization to 3D systems may introduce more interesting degeneracies such as knots and links [67].

K.Y., D.V., and E.J.B. acknowledge funding from the Swedish Research Council (VR) and the Knut and Alice Wallenberg Foundation. S.M. acknowledges funding from the Tsung-Dao Lee Institute. F.W. is supported in part by the U.S. Department of Energy under Grant No. DE-SC0012567, by the European Research Council under Grant No. 742104, and by the Swedish Research Council under Contract No.335-2014-7424.

[1] P. W. Anderson, The resonating valence bond state in La_2CuO_4 and superconductivity, Science **235**, 1196 (1987).
[2] L. Balents, Spin liquids in frustrated magnets, Nature (London) **464**, 199 (2010).
[3] L. Savary and L. Balents, Quantum spin liquids: A review, Rep. Prog. Phys. **80**, 016502 (2017).
[4] J. Knolle and R. Moessner, A field guide to spin liquids, Annu. Rev. Condens. Matter Phys. **10**, 451 (2019).
[5] K. Yang, S.-H. Phark, Y. Bae, T. Esat, P. Willke, A. Ardavan, A. J. Heinrich, and C. P. Lutz, Probing resonating valence bond states in artificial quantum magnets, Nat. Commun. **12**, 1 (2021).
[6] R. Sibille, E. Lhotel, M. Ciomaga Hatnean, G. J. Nilsen, G. Ehlers, A. Cervellino, E. Ressouche, M. Frontzek, O. Zaharko, V. Pomjakushin *et al.*, Coulomb spin liquid in anion-disordered pyrochlore $Tb_2Hf_2O_7$, Nat. Commun. **8**, 892 (2017).
[7] I. Kimchi, A. Nahum, and T. Senthil, Valence Bonds in Random Quantum Magnets: Theory and Application to $YbMgGaO_4$, Phys. Rev. X **8**, 031028 (2018).
[8] T.-H. Han, M. R. Norman, J.-J. Wen, J. A. Rodriguez-Rivera, J. S. Helton, C. Broholm, and Y. S. Lee, Correlated impurities and intrinsic spin-liquid physics in the kagome material herbertsmithite, Phys. Rev. B **94**, 060409 (2016)(R).
[9] H. B. Cao, A. Banerjee, J.-Q. Yan, C. A. Bridges, M. D. Lumsden, D. G. Mandrus, D. A. Tennant, B. C. Chakoumakos, and S. E. Nagler, Low-temperature crystal and magnetic structure of α-$RuCl_3$, Phys. Rev. B **93**, 134423 (2016).
[10] Z. Zhu, P. A. Maksimov, S. R. White, and A. L. Chernyshev, Disorder-Induced Mimicry of a Spin Liquid in $YbMgGaO_4$, Phys. Rev. Lett. **119**, 157201 (2017).
[11] Y. Li, D. Adroja, R. I. Bewley, D. Voneshen, A. A. Tsirlin, P. Gegenwart, and Q. Zhang, Crystalline Electric-Field Randomness in the Triangular Lattice Spin-Liquid $YbMgGaO_4$, Phys. Rev. Lett. **118**, 107202 (2017).
[12] C. M. Pasco, B. A. Trump, T. T. Tran, Z. A. Kelly, C. Hoffmann, I. Heinmaa, R. Stern, and T. M. McQueen, Single-crystal growth of $Cu_4(OH)_6BrF$ and universal behavior in quantum spin liquid candidates synthetic barlowite and herbertsmithite, Phys. Rev. Mater. **2**, 044406 (2018).
[13] S.-S. Lee, Low-energy effective theory of Fermi surface coupled with U(1) gauge field in $2+1$ dimensions, Phys. Rev. B **80**, 165102 (2009).
[14] D. F. Mross, J. McGreevy, H. Liu, and T. Senthil, Controlled expansion for certain non-fermi-liquid metals, Phys. Rev. B **82**, 045121 (2010).
[15] S.-S. Lee and P. A. Lee, U(1) Gauge Theory of the Hubbard Model: Spin Liquid States and Possible Application to κ-$(BEDT\text{-}TTF)_2Cu_2(CN)_3$, Phys. Rev. Lett. **95**, 036403 (2005).
[16] S. C. Morampudi, A. M. Turner, F. Pollmann, and F. Wilczek, Statistics of Fractionalized Excitations through Threshold Spectroscopy, Phys. Rev. Lett. **118**, 227201 (2017).
[17] S. C. Morampudi, F. Wilczek, and C. R. Laumann, Spectroscopy of Spinons in Coulomb Quantum Spin Liquids, Phys. Rev. Lett. **124**, 097204 (2020).
[18] S. D. Pace, S. C. Morampudi, R. Moessner, and C. R. Laumann, Emergent Fine Structure Constant of Quantum Spin Ice Is Large, Phys. Rev. Lett. **127**, 117205 (2021).
[19] E. J. Bergholtz, J. C. Budich, and F. K. Kunst, Exceptional topology of non-Hermitian systems, Rev. Mod. Phys. **93**, 015005 (2021).
[20] Z. Gong, Y. Ashida, K. Kawabata, K. Takasan, S. Higashikawa, and M. Ueda, Topological Phases of Non-Hermitian Systems, Phys. Rev. X **8**, 031079 (2018).
[21] H. Shen and L. Fu, Quantum Oscillation from In-Gap States and a Non-Hermitian Landau Level Problem, Phys. Rev. Lett. **121**, 026403 (2018).
[22] Y. Nagai, Y. Qi, H. Isobe, V. Kozii, and L. Fu, DMFT Reveals the Non-Hermitian Topology and Fermi Arcs in Heavy-Fermion Systems, Phys. Rev. Lett. **125**, 227204 (2020).
[23] M. Papaj, H. Isobe, and L. Fu, Nodal arc of disordered Dirac fermions and non-Hermitian band theory, Phys. Rev. B **99**, 201107(R) (2019).

[24] T. Matsushita, Y. Nagai, and S. Fujimoto, Disorder-induced exceptional and hybrid point rings in Weyl/Dirac semimetals, Phys. Rev. B **100**, 245205 (2019).

[25] A. A. Zyuzin and P. Simon, Disorder-induced exceptional points and nodal lines in Dirac superconductors, Phys. Rev. B **99**, 165145 (2019).

[26] T. Yoshida, R. Peters, N. Kawakami, and Y. Hatsugai, Exceptional band touching for strongly correlated systems in equilibrium, Prog. Theor. Exp. Phys. **2020**, 12A109 (2020).

[27] B. Michen, T. Micallo, and J. C. Budich, Exceptional non-Hermitian phases in disordered quantum wires, Phys. Rev. B **104**, 035413 (2021).

[28] L. Crippa, J. C. Budich, and G. Sangiovanni, Fourth-order exceptional points in correlated quantum many-body systems, Phys. Rev. B **104**, L121109 (2021).

[29] Y. Michishita, T. Yoshida, and R. Peters, Relationship between exceptional points and the Kondo effect in f-electron materials, Phys. Rev. B **101**, 085122 (2020).

[30] G. Jackeli and G. Khaliullin, Mott Insulators in the Strong Spin-Orbit Coupling Limit: From Heisenberg to a Quantum Compass and Kitaev Models, Phys. Rev. Lett. **102**, 017205 (2009).

[31] H. Takagi, T. Takayama, G. Jackeli, G. Khaliullin, and S. E. Nagler, Concept and realization of Kitaev quantum spin liquids, Nat. Rev. Phys. **1**, 264 (2019).

[32] A. Banerjee, J. Yan, J. Knolle, C. A. Bridges, M. B. Stone, M. D. Lumsden, D. G. Mandrus, D. A. Tennant, R. Moessner, and S. E. Nagler, Neutron scattering in the proximate quantum spin liquid α-RuCl3, Science **356**, 1055 (2017).

[33] K. Kitagawa, T. Takayama, Y. Matsumoto, A. Kato, R. Takano, Y. Kishimoto, S. Bette, R. Dinnebier, G. Jackeli, and H. Takagi, A spin–orbital-entangled quantum liquid on a honeycomb lattice, Nature (London) **554**, 341 (2018).

[34] Y. Kasahara, T. Ohnishi, Y. Mizukami, O. Tanaka, S. Ma, K. Sugii, N. Kurita, H. Tanaka, J. Nasu, Y. Motome *et al.*, Majorana quantization and half-integer thermal quantum Hall effect in a Kitaev spin liquid, Nature (London) **559**, 227 (2018).

[35] Y. Vinkler-Aviv and A. Rosch, Approximately Quantized Thermal Hall Effect of Chiral Liquids Coupled to Phonons, Phys. Rev. X **8**, 031032 (2018).

[36] M. Ye, G. B. Halász, L. Savary, and L. Balents, Quantization of the Thermal Hall Conductivity at Small Hall Angles, Phys. Rev. Lett. **121**, 147201 (2018).

[37] J. G. Rau, E. K.-H. Lee, and H.-Y. Kee, Spin-orbit physics giving rise to novel phases in correlated systems: Iridates and related materials, Annu. Rev. Condens. Matter Phys. **7**, 195 (2016).

[38] M. Gohlke, G. Wachtel, Y. Yamaji, F. Pollmann, and Y. B. Kim, Quantum spin liquid signatures in Kitaev-like frustrated magnets, Phys. Rev. B **97**, 075126 (2018).

[39] M. Hermanns, I. Kimchi, and J. Knolle, Physics of the Kitaev model: Fractionalization, dynamic correlations, and material connections, Annu. Rev. Condens. Matter Phys. **9**, 17 (2018).

[40] M. Berry, Physics of nonhermitian degeneracies, Czech. J. Phys. **54**, 1039 (2004).

[41] K. Yang, S. C. Morampudi, and E. J. Bergholtz, Exceptional Spin Liquids from Couplings to the Environment, Phys. Rev. Lett. **126**, 077201 (2021).

[42] M. Peskin, *An Introduction To Quantum Field Theory* (CRC Press, Boca Raton, FL, 2018).

[43] X. Wen, *Quantum Field Theory of Many-Body Systems: From the Origin of Sound to an Origin of Light and Electrons*, Oxford Graduate Texts (Oxford University Press, Oxford, U.K., 2007).

[44] K. Kawabata, K. Shiozaki, M. Ueda, and M. Sato, Symmetry and Topology in Non-Hermitian Physics, Phys. Rev. X **9**, 041015 (2019).

[45] J. C. Budich, J. Carlström, F. K. Kunst, and E. J. Bergholtz, Symmetry-protected nodal phases in non-Hermitian systems, Phys. Rev. B **99**, 041406(R) (2019).

[46] T. Yoshida, R. Peters, N. Kawakami, and Y. Hatsugai, Symmetry-protected exceptional rings in two-dimensional correlated systems with chiral symmetry, Phys. Rev. B **99**, 121101(R) (2019).

[47] A. Kitaev, Anyons in an exactly solved model and beyond, Ann. Phys. **321**, 2 (2006).

[48] See Supplemental Material at http://link.aps.org/supplemental/10.1103/PhysRevResearch.4.L042025 for details of symmetry transformation, degeneracy for Dirac fermions, calculations of correlation functions, random magnetic field realizations and numerical disordered results.

[49] A. J. Willans, J. T. Chalker, and R. Moessner, Disorder in a Quantum Spin Liquid: Flux Binding and Local Moment Formation, Phys. Rev. Lett. **104**, 237203 (2010).

[50] A. J. Willans, J. T. Chalker, and R. Moessner, Site dilution in the Kitaev honeycomb model, Phys. Rev. B **84**, 115146 (2011).

[51] D. Otten, A. Roy, and F. Hassler, Dynamical structure factor in the non-Abelian phase of the Kitaev honeycomb model in the presence of quenched disorder, Phys. Rev. B **99**, 035137 (2019).

[52] F. Zschocke and M. Vojta, Physical states and finite-size effects in Kitaev's honeycomb model: Bond disorder, spin excitations, and NMR line shape, Phys. Rev. B **92**, 014403 (2015).

[53] J. Knolle, R. Moessner, and N. B. Perkins, Bond-Disordered Spin Liquid and the Honeycomb Iridate $H_3LiIr_2O_6$: Abundant Low-Energy Density of States from Random Majorana Hopping, Phys. Rev. Lett. **122**, 047202 (2019).

[54] A. Weiße, G. Wellein, A. Alvermann, and H. Fehske, The kernel polynomial method, Rev. Mod. Phys. **78**, 275 (2006).

[55] D. Varjas, M. Fruchart, A. R. Akhmerov, and P. M. Perez-Piskunow, Computation of topological phase diagram of disordered $Pb_{1-x}Sn_xTe$ using the kernel polynomial method, Phys. Rev. Res. **2**, 013229 (2020).

[56] K. Feng, N. B. Perkins, and F. J. Burnell, Further insights into the thermodynamics of the Kitaev honeycomb model, Phys. Rev. B **102**, 224402 (2020).

[57] W.-H. Kao, J. Knolle, G. B. Halász, R. Moessner, and N. B. Perkins, Vacancy-Induced Low-Energy Density of States in the Kitaev Spin Liquid, Phys. Rev. X **11**, 011034 (2021).

[58] A. Metavitsiadis, W. Natori, J. Knolle, and W. Brenig, Optical phonons coupled to a Kitaev spin liquid, Phys. Rev. B **105**, 165151 (2022).

[59] A. Metavitsiadis and W. Brenig, Phonon renormalization in the Kitaev quantum spin liquid, Phys. Rev. B **101**, 035103 (2020).

[60] M. Ye, R. M. Fernandes, and N. B. Perkins, Phonon dynamics in the kitaev spin liquid, Phys. Rev. Res. **2**, 033180 (2020).

[61] X.-Y. Song, Y.-Z. You, and L. Balents, Low-Energy Spin Dynamics of the Honeycomb Spin Liquid Beyond the Kitaev Limit, Phys. Rev. Lett. **117**, 037209 (2016).

[62] Y. Wan and N. P. Armitage, Resolving Continua of Fractional Excitations by Spinon Echo in THz 2D Coherent Spectroscopy, Phys. Rev. Lett. **122**, 257401 (2019).

[63] W. Choi, K. H. Lee, and Y. B. Kim, Theory of Two-Dimensional Nonlinear Spectroscopy for the Kitaev Spin Liquid, Phys. Rev. Lett. **124**, 117205 (2020).

[64] R. M. Nandkishore, W. Choi, and Y. B. Kim, Spectroscopic fingerprints of gapped quantum spin liquids, both conventional and fractonic, Phys. Rev. Res. **3**, 013254 (2021).

[65] M. Kanega, T. N. Ikeda, and M. Sato, Linear and nonlinear optical responses in Kitaev spin liquids, Phys. Rev. Res. **3**, L032024 (2021).

[66] Z.-L. Li, M. Oshikawa, and Y. Wan, Photon Echo from Lensing of Fractional Excitations in Tomonaga-Luttinger Spin Liquid, Phys. Rev. X **11**, 031035 (2021).

[67] J. Carlström, M. Stålhammar, J. C. Budich, and E. J. Bergholtz, Knotted non-Hermitian metals, Phys. Rev. B **99**, 161115(R) (2019).